Interaction of Bis(1,2,6,7-tetracyano-3,5-dihydro-3,5-diiminopyrrolizinide) Metal Complexes with Phenazine and Derivatives. Crystal Structures of Addition Compounds of the Nickel(II) Complex with Phenazine and 5,10-Dimethyl-5,10-dihydrophenazine

Mario Bonamico,[a] Vincenzo Fares,*[,a] Alberto Flamini,*[,a] Nicola Poli,[a] Yoshiro Yamashita[b] and Kenichi Imaeda[b]

[a] *Istituto di Chimica dei Materiali, Area della Ricerca di Roma, PO Box 10, 00016 Monterotondo Stazione, Roma, Italy*

[b] *Chemical Materials Center, Institute for Molecular Science, Okazaki, 444 Japan*

The charge-transfer compounds of the electron-acceptor moiety $[NiL_2]$ (L = 1,2,6,7-tetracyano-3,5-dihydro-3,5-diiminopyrrolizinide) and the electron-donating phenazine derivatives [phenazine (phz), 5,10-dimethyl-5,10-dihydrophenazine (dmphz) and *N*-methylphenazinium cation ($mphz^+$)] have been synthesized and characterized. The X-ray crystal structures of $[NiL_2]$·2phz·2MeCN **1a** and $[NiL_2]$·dmphz·2MeCN **1b** have been determined. Both compounds are monoclinic, mixed-stacked compounds, with planar acceptor and donor moieties alternating along the *c* axis [**1a**: space group $P2_1/n$, $a = 14.687(1)$, $b = 21.364(2)$, $c = 7.8208(6)$ Å, $\beta = 110.958(6)°$, $Z = 2$; **1b**: space group $P2_1/c$, $a = 12.975(5)$, $b = 19.838(7)$, $c = 7.651(3)$ Å, $\beta = 106.05(2)°$, $Z = 2$]. While **1a**, as expected, does not show any solid-state collective property, **1b** is a semiconductor (single crystal $\rho = 3.6 \times 10^3$ Ω cm at room temperature; $E_a = 0.28$ eV); its degree of ionicity gradually increases, on lowering the temperature, from zero to a small amount corresponding to an effective magnetic moment (μ_{eff}) = of 0.28 μ_B per molecular formula. The cobalt derivative $[CoL_2]$·dmphz·2MeCN has also been synthesized and characterized, which is isomorphous and isostructural with the nickel analogue, and qualitatively behaves likewise (single crystal $\rho = 4.2 \times 10^5$ Ω cm at room temperature; $E_a = 0.26$ eV); its magnetic measurements show a high-spin metal configuration ($S = \frac{3}{2}$, $\mu_{eff} = 4.13$ μ_B). The *N*-methylphenazinium ($mphz^+$) derivative, isolated as $[NiL_2]^{\bullet-}$·$mphz^+$·2MeOH, is assumed to be a mixed-stacked radical anion salt from magnetic (μ_{eff} = 1.72 μ_B) and electrical (powder $\rho = 5.5 \times 10^6$ Ω cm at room temperature, $E_a = 0.43$ eV) measurements.

We are currently investigating the relationship between physical properties and structure in solid donor–acceptor compounds of the metal complexes $[ML_2]$ which are electron acceptor molecules. The specific interest in these species, which are derived from tetracyanoethylene,[1] is the close similarity with the popular compound tetracyanoquinodimethane (tcnq), given the presence of the high number of substituent C≡N groups. In spite of this formal resemblance, the two systems exhibit two different cyclovoltammetric properties, which are believed to greatly affect the solid-state electrical properties of the donor–acceptor complexes derived from them: (*i*) $[ML_2]$ complexes are reduced at a more negative electrode potential than tcnq itself ($\Delta E_{\frac{1}{2}} = 0.53$ or 0.13 V, for Fe[2] or Pd[3] respectively) and (*ii*) the difference between the first and the second reduction potential is smaller for $[ML_2]$ than for tcnq [0.09 *vs.* 0.46 V (M = Ni)].

Our previous studies were concerned with adducts of $[NiL_2]$, with tetrathiafulvalene (ttf) and the crystallization solvent tetrahydrofuran (thf)[1] and, after electrochemical reduction in methanol, the tetraethylammonium cation.[1] The complex $[NiL_2]$ttf·2thf is diamagnetic and an insulator, containing alternate arrangements of donor–acceptor neutral molecules, while $[NiL_2]^{\bullet-}$·NEt_4^+·4MeOH is a simple radical anion salt, a semiconductor ($\rho = 0.94 \times 10^4$ Ω cm at room temperature), probably containing stacks of segregated anions, partially antiferromagnetically coupled ($\mu_{eff} = 1.36$ μ_B at room temperature). We have recently turned to the study of charge-transfer (c.t.) complexes of $[NiL_2]$ with phenazine compounds, *i.e.* phenazine (phz), 5,10-dimethyl-5,10-dihydrophenazine (dmphz) and the *N*-methylphenazinium cation ($mphz^+$). In this paper the results of these studies are reported and the properties of the new complexes compared with those of the analogous well known c.t. tcnq complexes. The crystal structures of the addition compounds of $[NiL_2]$ with phz or dmphz and acetonitrile, $[NiL_2]$·2phz·2MeCN **1a** and $[NiL_2]$·dmphz·2MeCN **1b**, are described. The results on the homologous complex $[CoL_2]$, with dmphz $[CoL_2]$·dmphz·2MeCN **2b** are also reported.

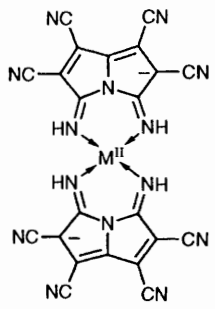

$[ML_2]$

† *Supplementary data available:* see Instructions for Authors, *J. Chem. Soc., Dalton Trans.*, 1993, Issue 1, pp. xxiii–xxviii.

Non-SI units employed: eV ≈ 1.60×10^{-19} J, G = 10^{-4} T, emu = $10^6/4\pi$ SI, $\mu_B \approx 9.274\,02 \times 10^{-24}$ J T^{-1}.

Results and Discussion

Crystal Structures of **1a** *and* **1b**.—Complexes **1a** and **1b** belong to the same class (π-molecular compounds) as $[NiL_2]$·ttf·2thf[1] **1c**, of general formula $[NiL_2]$·X·2A, where A is an equatorial solvent molecule capable of forming hydrogen bonds with the ligand imino groups (Fig. 1), and X is a planar, extensively conjugated donor molecule. All show the same general structural features, consisting essentially of an infinite mixed stack of alternating planar $[NiL_2]$ and X moieties, along the *c* axis (Figs. 2 and 3), with intrastack interplanar distances of 3.26 (**1a**), 3.35 (**1b**) and 3.46 Å (**1c**), and an inclination angle with the *z* direction of *ca.* 58, 59 and 60° respectively.

The structural similarity is greater between **1b** and **1c**, where only one X molecule is present per nickel complex, in both cases lying on a centre of symmetry at 0, 0, $\frac{1}{2}$. In the case of derivative **1a** there are two symmetry-related (through the same centre of symmetry) phenazine molecules per complex unit.

There is a notable difference in the degree of superposition of $[NiL_2]$ and X units in **1a** and **1b**: in the latter, the molecular long axes have the same orientation, and all three conjugated rings of dmphz overlap with the complex unit (Fig. 4), while in the former such axes are at almost 45° to each other, and only two phenazine aromatic rings are involved in the overlapping (Fig. 5). Moreover, a phenazine nitrogen atom in **1a** lies on the nickel apical position at a distance Ni–N(101) of 3.31 Å, resembling that found in the ttf derivative **1c**, with a Ni–ttf distance of 3.51 Å, while in compound **1b** the nickel apical position is occupied by the dmphz ring-carbon atom C(106) at a

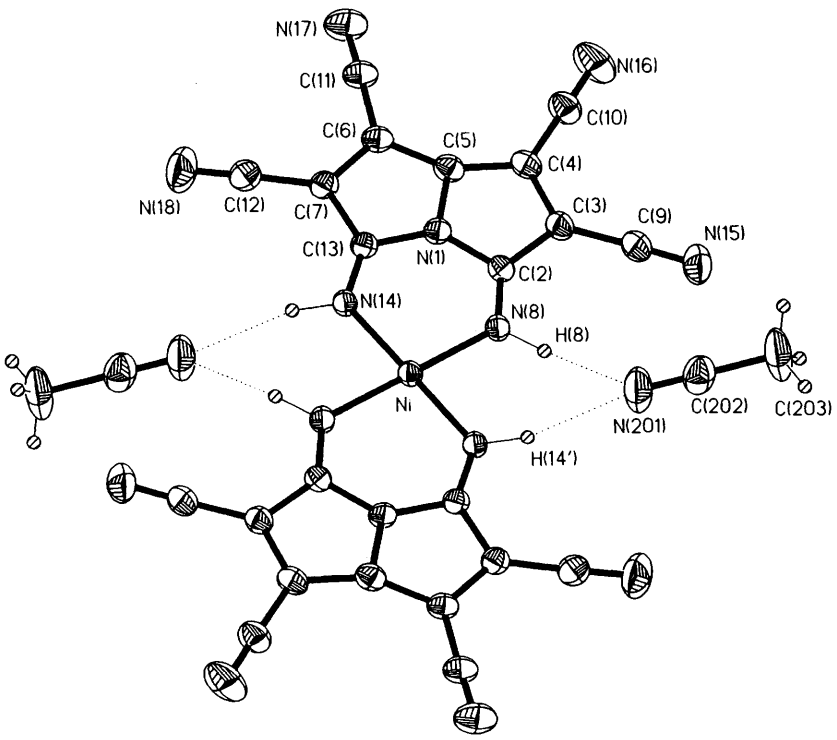

Fig. 1 Perspective drawing and labelling scheme of the $[NiL_2]$ complex units, together with the equatorial acetonitrile molecules, present in both **1a**, **1b** and analogous compounds. Thermal ellipsoids are at the 30% probability level

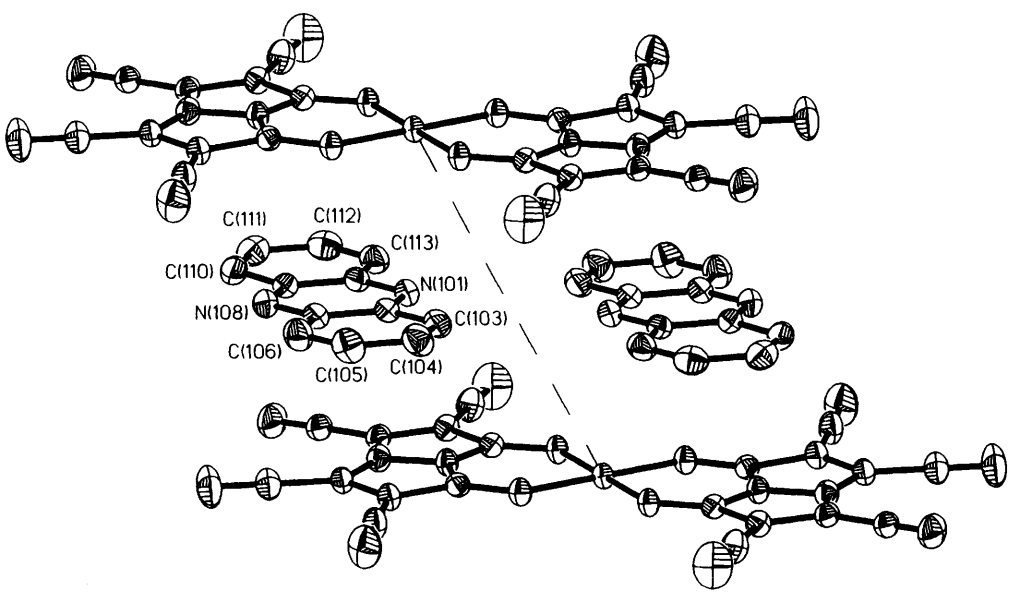

Fig. 2 A partial schematic view of compound **1a**, showing the mixed stack of the $[NiL_2]$ complex and phenazine units developing along the *c* axis (dashed line). The acetonitrile molecules and the hydrogen atoms have been omitted for clarity

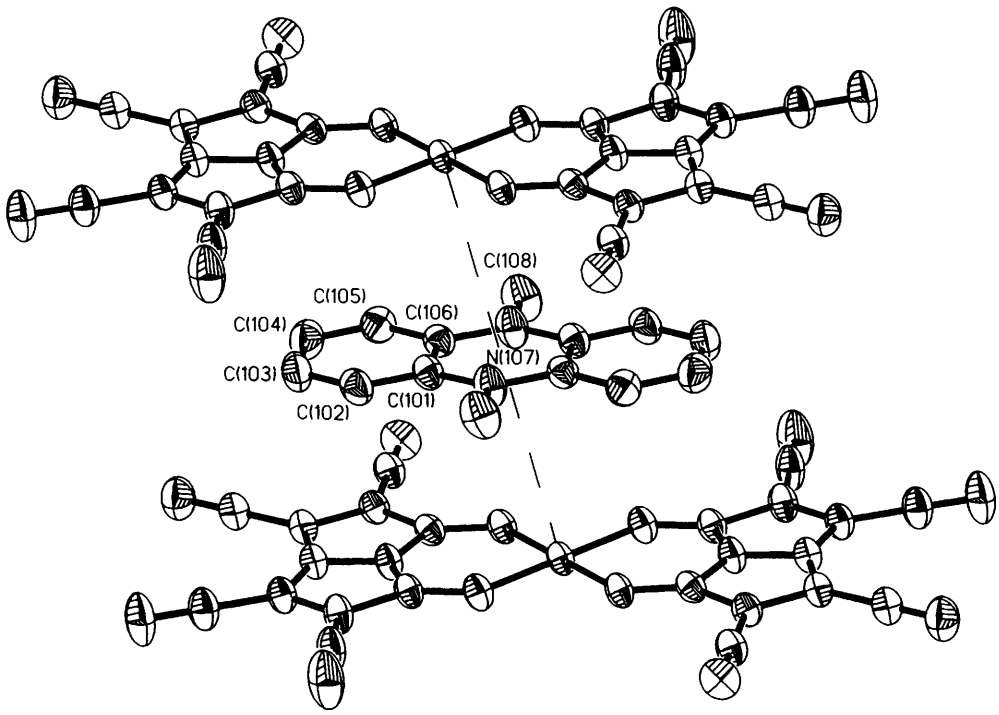

Fig. 3 Alternating planar, centrosymmetrical, nickel complex and dmphz units stacked along the *c* axis (dashed line) in compound **1b**

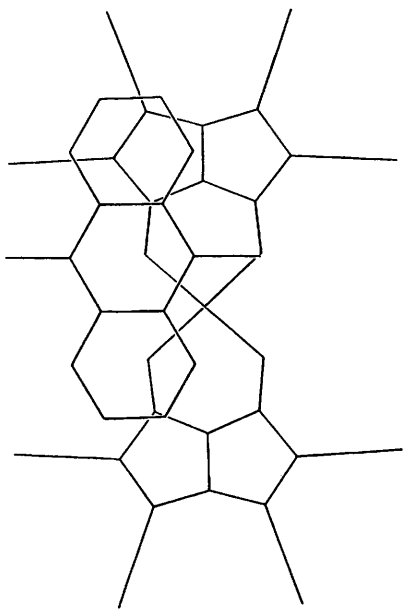

Fig. 4 A schematic projection onto the molecular plane of the nickel complex and dmphz units of compound **1b**, showing the poorly charged central part of the three conjugated dmphz rings overlapping with the highly charged nitrogen and carbon atoms of the complex

distance of 3.41 Å. The observed structural differences, due to the different electronic distribution in the 16 π-electron strong-donor dmphz and the 14 π-electron weak-donor phz,[4a] easily explain the different solid-state cooperative properties of **1a** and **1b** (see below).

Tables 1 and 2 contain the atomic coordinates and Tables 3 and 4 selected bond lengths and angles for compounds **1a** and **1b** respectively. As already found in the analogous ttf derivative **1c**, in both **1a** and **1b** the nickel atom is symmetrically surrounded by four imino groups from two chelating ligands in a square-planar arrangement (Fig. 1). The Ni–N distances, and the bond distances and angles within the heterocyclic ligand, are strictly comparable in the two compounds, as expected, given the structural similarity outlined above, and can be

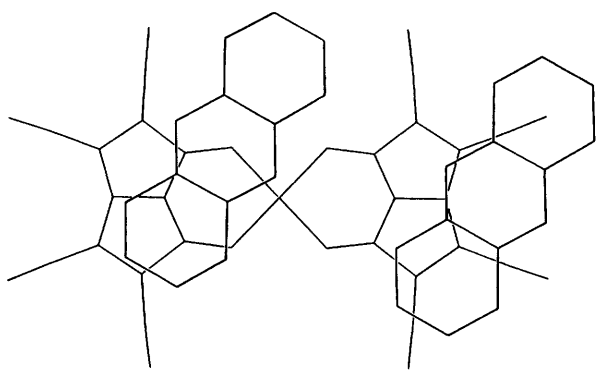

Fig. 5 A schematic drawing of the $[NiL_2]$ complex and phenazine molecules of compound **1a**, projected onto the molecular plane: only two phenazine aromatic rings partially overlap with the complex

related to the metal co-ordination geometry, as noted elsewhere.[1] Only slight differences can be found for the hydrogen-bond interactions of the equatorial acetonitrile molecules with the metal-co-ordinated imino groups, N(acetonitrile)···H(imino) distances being 2.13 and 2.16 Å in **1a** and 2.20 and 2.22 Å in **1b**.

The molecular details of the phenazine unit in **1a** and 5,10-dimethyl-5,10-dihydrophenazine in **1b** are strictly comparable both with those observed in the tcnq–phz[4b] and tcnq–dmphz[5a] derivatives, and with other literature data.[6–8] It is noticeable, however, that whilst in tcnq–dmphz derivatives the dmphz molecules, partially negatively charged (*ca.* −0.5),[5b] is bent, in the present case the uncharged dmphz is planar (by symmetry), the mean deviation from the least-squares plane (methyl groups excluded) being 0.013 Å.

Solid-state Properties.—$[NiL_2]$·2phz·2MeCN **1a**. Compound **1a** does not show any solid-state collective property, or any electronic intermolecular interactions between $[NiL_2]$ and phenazine. It is an insulator, diamagnetic, ESR silent and has no ligand-field absorption below 10 000 cm^{-1} in the reflectance spectrum, diagnostic of axial co-ordination to the metal, which is in fact extremely weak, or non-existent, given the long N(phz)···Ni distance (3.31 Å).

Table 1 Atomic coordinates ($\times 10^4$) with estimated standard deviations (e.s.d.s) in parentheses, of non-hydrogen atoms for compound **1a**

Atom	*x*	*y*	*z*
Ni	0	0	0
N(1)	1893(2)	244(1)	856(4)
C(2)	1479(2)	776(2)	498(4)
C(3)	2139(2)	1271(2)	584(5)
C(4)	2903(2)	997(2)	1006(4)
C(5)	2747(3)	348(2)	1169(5)
C(6)	3081(3)	248(2)	1426(4)
C(7)	2414(2)	694(2)	1283(4)
N(8)	686(2)	737(1)	143(4)
C(9)	2024(3)	1908(2)	221(6)
C(10)	3700(3)	1323(2)	1240(5)
C(11)	3962(3)	385(2)	1750(5)
C(12)	2441(3)	1350(2)	1505(5)
C(13)	1644(2)	369(2)	887(4)
N(14)	885(2)	535(1)	539(3)
N(15)	1929(3)	2414(2)	117(6)
N(16)	4337(3)	1573(2)	1432(6)
N(17)	4663(2)	503(2)	1972(5)
N(18)	2424(3)	1878(2)	1688(6)
N(101)	1274(2)	95(1)	4433(4)
C(102)	1177(3)	717(2)	4540(4)
C(103)	361(3)	960(2)	4886(5)
C(104)	248(3)	1593(2)	4965(6)
C(105)	935(3)	2008(2)	4740(6)
C(106)	1732(3)	1796(2)	4432(5)
C(107)	1886(3)	1140(2)	4312(4)
N(108)	2657(2)	938(1)	3962(4)
C(109)	2754(3)	312(2)	3846(4)
C(110)	3557(3)	65(2)	3453(5)
C(111)	3655(3)	561(2)	3299(5)
C(112)	2953(3)	975(2)	3534(5)
C(113)	2177(3)	759(2)	3906(5)
C(114)	2044(3)	106(2)	4067(4)
N(201)	538(3)	1905(2)	312(6)
C(202)	491(3)	2414(2)	602(6)
C(203)	410(4)	3084(2)	987(9)

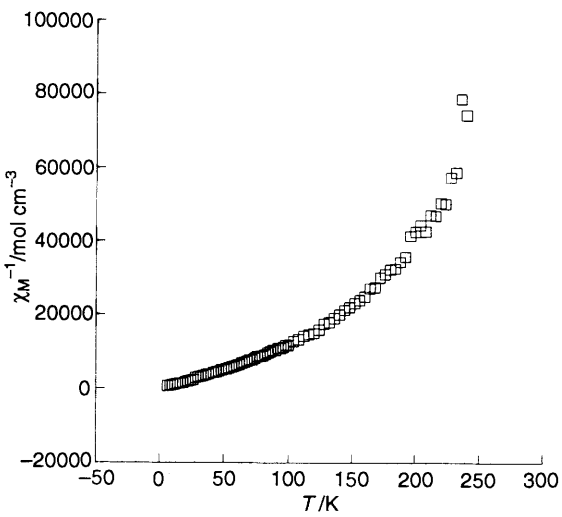

Fig. 6 Temperature dependence of the reciprocal molar susceptibility for compound **1b**

[NiL_2]·dmphz·2MeCN **1b**. Compound **1b** is a largely neutral molecular complex, because of the very small paramagnetism at 300 K. Accordingly, at room temperature it exhibits a weak, structureless and exchange-broadened (100 G) EPR single resonance (Table 5), indicative of a low concentration of unpaired spins, rapidly moving along the chains. However, the temperature dependence of the molar susceptibility (χ_M) is quite anomalous (Fig. 6); χ_M is positive and vanishingly small at room temperature, as expected, but its reciprocal decreases

Table 2 Atomic coordinates ($\times 10^4$) with e.s.d.s in parentheses of non-hydrogen atoms for compound **1b**

Atom	*x*	*y*	*z*
Ni	0	0	0
N(1)	2074(2)	782(1)	−92(4)
C(2)	2266(3)	196(2)	867(5)
C(3)	3429(3)	165(2)	1516(5)
C(4)	3836(3)	729(2)	864(5)
C(5)	2979(3)	1122(2)	−169(5)
C(6)	2636(3)	1689(2)	−1262(5)
C(7)	1504(3)	1679(2)	−1819(5)
N(8)	1471(2)	−175(1)	987(4)
C(9)	4005(3)	−348(2)	2629(7)
C(10)	4942(3)	904(2)	1203(6)
C(11)	3291(3)	2167(2)	−1802(6)
C(12)	822(3)	2156(2)	−2972(6)
C(13)	1140(3)	1090(2)	−1057(5)
N(14)	224(2)	821(1)	−1094(4)
N(15)	4462(3)	−765(2)	3541(8)
N(16)	5830(3)	1045(2)	1456(7)
N(17)	3819(3)	2554(2)	−2237(6)
N(18)	287(3)	2535(2)	−3914(5)
C(101)	1126(3)	26(2)	5453(5)
C(102)	2226(3)	71(2)	5867(6)
C(103)	2712(4)	616(3)	5313(7)
C(104)	2121(4)	1110(3)	4286(7)
C(105)	1019(3)	1075(2)	3861(6)
C(106)	508(3)	548(2)	4430(5)
N(107)	−607(2)	523(2)	4030(5)
C(108)	−1229(4)	1095(2)	3047(8)
N(201)	−1915(3)	1582(3)	−2773(8)
C(202)	−2616(5)	1904(3)	−3525(10)
C(203)	−3580(6)	2289(4)	−4536(13)

more steeply than predicted by the Curie law down to 100 K and then linearly from 100 to 4 K with $\mu_{eff} = 0.28\ \mu_B$ per molecular formula. Moreover, the integrated intensity of the EPR absorption increases by a factor of ten on going from 300 to 77 K while remaining structureless and broad (120 G), in qualitative agreement with the results of bulk susceptibility measurements. Such behaviour cannot be due in any part to paramagnetic chemical impurities for two reasons; first, since freshly prepared samples of [NiL_2]·2MeCN and dmphz did not contain any detectable free radical, and secondly since the related cobalt complex, reported below, exhibits a similar behaviour. The reason might be instead an increase in concentration, on lowering the temperature, of the radicals $[NiL_2]^{\bullet -}$ and $dmphz^{\bullet +}$, arising from a shift to the right of the dynamic equilibrium in the solid state, *i.e.* [NiL_2]·dmphz $\rightleftharpoons$ $[NiL_2]^{\bullet -}$ + $dmphz^{\bullet +}$. On the other hand the corresponding E_{ct} and $\Delta E_{o,r}$ values (Table 5) suggest that **1b** lies near the neutral–ionic boundary in the empirical V-shape Torrance diagram,[9] which correlates the above-measured parameters with the degree of ionicity for a broad range of different mixed-stacked c.t. complexes. Therefore this compound can undergo a variation of ionicity, induced by pressure or temperature, as in previously studied quasi-neutral mixed-stack solids.[9,10] Usually such materials change discontinuously from neutral to ionic on lowering the temperature; in contrast, **1b** gradually changes with no break either in the χ_M^{-1} *vs.* *T* curve or in the plot of log ρ against $10^3\ T^{-1}$, the slope of which remains constant (Fig. 7). Such behaviour is also remarkably different from that of the related compound tcnq·dmphz. Although the latter is largely diamagnetic at room temperature with a weak EPR signal ($g = 2.0026$)[11] (as for **1b**) and a semiconductor with a comparable value of resistivity ($\rho = 6 \times 10^4\ \Omega$ cm),[12] its magnetic susceptibility is thermally activated below 350 K and the activation energy for conductivity is consequently higher (0.51 eV).[11]

[CoL_2]·dmphz·2MeCN **2b**. Qualitatively compound **2b** behaves similarly to the previous nickel complex, the only

Table 3 Selected bond lengths (Å) and angles (°) with e.s.d.s in parentheses for compound **1a**

Ni–N(8)	1.894(3)	C(13)–N(14)	1.288(4)
Ni–N(14)	1.888(3)	N(101)–C(102)	1.343(5)
N(1)–C(2)	1.364(4)	N(101)–C(114)	1.333(4)
N(1)–C(5)	1.379(4)	C(102)–C(103)	1.417(5)
N(1)–C(13)	1.359(4)	C(102)–C(107)	1.437(5)
C(2)–C(3)	1.453(5)	C(103)–C(104)	1.364(6)
C(2)–N(8)	1.292(4)	C(104)–C(105)	1.404(6)
C(3)–C(4)	1.407(5)	C(105)–C(106)	1.355(6)
C(3)–C(9)	1.411(5)	C(106)–C(107)	1.427(5)
C(4)–C(5)	1.403(5)	C(107)–N(108)	1.329(5)
C(4)–C(10)	1.429(5)	N(108)–C(109)	1.352(5)
C(5)–C(6)	1.406(5)	C(109)–C(110)	1.421(5)
C(6)–C(7)	1.397(5)	C(109)–C(114)	1.430(5)
C(6)–C(11)	1.436(5)	C(110)–C(111)	1.358(6)
C(7)–C(12)	1.416(5)	C(111)–C(112)	1.418(6)
C(7)–C(13)	1.452(5)	C(112)–C(113)	1.353(6)
C(9)–N(15)	1.134(5)	C(113)–C(114)	1.422(5)
C(10)–N(16)	1.133(6)	N(201)–C(202)	1.118(6)
C(11)–N(17)	1.132(5)	C(202)–C(203)	1.477(6)
C(12)–N(18)	1.135(6)		
N(14)–Ni–N(8)	93.8(1)	C(107)–C(102)–C(103)	119.5(3)
C(5)–N(1)–C(2)	113.8(3)	C(104)–C(103)–C(102)	119.9(4)
C(13)–N(1)–C(2)	132.0(3)	C(105)–C(104)–C(103)	121.1(4)
C(13)–N(1)–C(5)	114.1(3)	C(106)–C(105)–C(104)	121.0(4)
C(3)–C(2)–N(1)	104.0(3)	C(107)–C(106)–C(105)	120.5(4)
N(8)–C(2)–N(1)	119.5(3)	C(106)–C(107)–C(102)	118.1(3)
C(4)–C(3)–C(2)	108.0(3)	N(108)–C(107)–C(102)	122.1(3)
C(5)–C(4)–C(3)	108.4(3)	C(109)–N(108)–C(107)	116.9(3)
C(4)–C(5)–N(1)	105.8(3)	C(114)–C(109)–N(108)	120.7(3)
C(6)–C(5)–N(1)	105.4(3)	C(114)–C(109)–C(110)	119.5(3)
C(7)–C(6)–C(5)	108.4(3)	C(111)–C(110)–C(109)	120.5(4)
C(13)–C(7)–C(6)	108.3(3)	C(112)–C(111)–C(110)	119.9(4)
C(2)–N(8)–Ni	127.3(2)	C(113)–C(112)–C(111)	121.4(4)
C(7)–C(13)–N(1)	103.8(3)	C(114)–C(113)–C(112)	120.6(4)
N(14)–C(13)–N(1)	120.7(3)	C(109)–C(114)–N(101)	122.5(3)
C(13)–N(14)–Ni	126.7(2)	C(113)–C(114)–C(109)	118.1(3)
C(114)–N(101)–C(102)	116.7(3)	C(203)–C(202)–N(201)	178.8(6)
C(107)–C(102)–N(101)	121.1(3)		

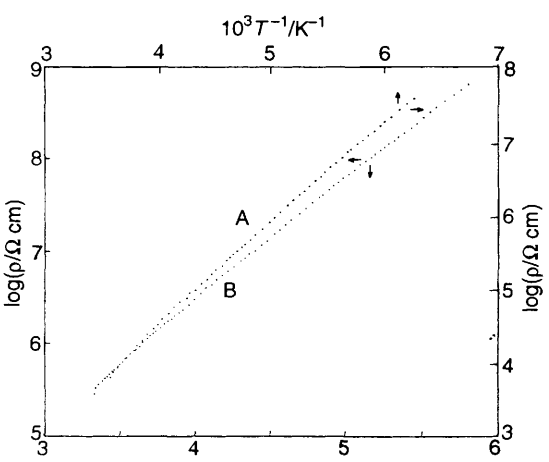

Fig. 7 Temperature dependence of the specific electrical resistivity for single crystals of **1b** (A) and **2b** (B)

difference being that the ionization equilibrium in the solid state is shifted more to the left, as expected from the larger $\Delta E_{o,r}$ value (Table 5). Accordingly, the structureless and broad (160 G) EPR signal is weaker, its integrated intensity increases by a factor of three on lowering the temperature from 300 to 77 K, and the electrical resistivity is also higher (Fig. 7). The magnetic susceptibility, which is dominated by the metal-centred unpaired electrons, deserves comment. The plot of $\chi_M(T)$ exhibits a strict conformity to the Curie law down to 4 K, with a

Table 4 Selected bond lengths (Å) and angles (°) with e.s.d.s in parentheses for compound **1b**

Ni–N(8)	1.881(3)	C(10)–N(16)	1.148(5)
Ni–N(14)	1.889(3)	C(11)–N(17)	1.138(6)
N(1)–C(2)	1.360(5)	C(12)–N(18)	1.136(5)
N(1)–C(5)	1.370(5)	C(13)–N(14)	1.297(5)
N(1)–C(13)	1.375(4)	C(101)–C(102)	1.377(6)
C(2)–C(3)	1.453(5)	C(101)–C(106)	1.408(5)
C(2)–N(8)	1.291(5)	C(101)–N(107′)	1.394(5)
C(3)–C(4)	1.388(6)	C(102)–C(103)	1.377(8)
C(3)–C(9)	1.403(6)	C(103)–C(104)	1.353(7)
C(4)–C(5)	1.408(5)	C(104)–C(105)	1.377(7)
C(4)–C(10)	1.429(5)	C(105)–C(106)	1.371(6)
C(5)–C(6)	1.398(5)	C(106)–N(107)	1.394(5)
C(6)–C(7)	1.412(5)	N(107)–C(108)	1.473(6)
C(6)–C(11)	1.410(6)	N(107)–C(101′)	1.394(5)
C(7)–C(12)	1.423(5)	N(201)–C(202)	1.130(7)
C(7)–C(13)	1.442(5)	C(202)–C(203)	1.487(10)
C(9)–N(15)	1.138(6)		
N(8)–Ni–N(14)	94.2(1)	C(7)–C(12)–N(18)	178.8(5)
C(2)–N(1)–C(5)	114.4(3)	N(1)–C(13)–C(7)	103.9(3)
C(2)–N(1)–C(13)	132.3(3)	N(1)–C(13)–N(14)	119.6(3)
C(5)–N(1)–C(13)	113.3(3)	Ni–N(14)–C(13)	126.7(2)
N(1)–C(2)–C(3)	103.8(3)	C(102)–C(101)–C(106)	118.4(4)
N(1)–C(2)–N(8)	119.6(3)	C(106)–C(101)–N(107′)	119.1(3)
C(2)–C(3)–C(4)	107.8(3)	C(101)–C(102)–C(103)	120.9(4)
C(3)–C(4)–C(5)	109.1(3)	C(102)–C(103)–C(104)	120.9(4)
N(1)–C(5)–C(4)	104.8(3)	C(103)–C(104)–C(105)	119.0(5)
N(1)–C(5)–C(6)	106.7(3)	C(104)–C(105)–C(106)	121.7(4)
C(5)–C(6)–C(7)	107.6(3)	C(101)–C(106)–C(105)	119.1(3)
C(6)–C(7)–C(13)	108.5(3)	C(101)–C(106)–N(107)	119.5(3)
Ni–N(8)–C(2)	127.5(2)	C(106)–N(107)–C(108)	118.2(3)
C(3)–C(9)–N(15)	179.2(6)	C(106)–N(107)–C(101′)	121.3(3)
C(4)–C(10)–N(16)	179.3(5)	C(108)–N(107)–C(101′)	120.5(3)
C(6)–C(11)–N(17)	180.0(7)	N(201)–C(202)–C(203)	176.4(7)

Primed atoms related to corresponding unprimed atoms by the symmetry code $-x, -y, 1-z$.

temperature-independent μ_{eff} value (4.13 μ_B), nearly the same as the spin-only value for three unpaired electrons (3.88 μ_B); no EPR absorption, attributable to these electrons, was obtained even at liquid-nitrogen temperature, probably because of the occurrence of a very short spin-lattice relaxation time, as is usual in high-spin Co^{II} complexes.[13] Given the planarity of $[CoL_2]$ by symmetry and the absence of any tetragonal-field component, this example must be regarded as an exceptional, structurally characterized, square-planar high-spin ($S = \frac{3}{2}$) Co^{II} complex, confirming that the tetracyanodiiminopyrrolizinide ligand provides a weak ligand field.[2] However, further investigations are needed, such as EPR measurements at liquid-helium temperature on neat **2b** and/or diluted in **1b**, in order to ascertain that the ground state is a quartet state, eventually lying just below an excited doublet state, in a situation which is the reverse of that most widely occurring in square-planar Co^{II} complexes.[14]

$[NiL_2]^{\bullet-}$·$mphz^+$·2MeOH **1d**. We decided to synthesize this compound in the hope of obtaining an organic metal-like conductor, by analogy with the well known compound $tcnq^{\bullet-}$·$mphz^+$, which has a uniform segregated-stack crystal structure[15a] and exhibits a metallic state above 200 K.[15b] Compound **1d** was prepared after galvanostatic reduction of $[NiL_2]$ in the presence of a large excess of *N*-methylphenazinium methanesulfate; the electrolysis was stopped after the colour of the solution had changed from dark to light green and the cathode surface was completely covered with a black microcrystalline solid. During the electrolysis, the neutral *N*-methylphenazinyl radical, mphz$^{\bullet}$, is mainly formed because $mphz^+$ is more easily reduced than $[NiL_2]$ ($E_{pc} = -0.11$[16] and -0.22[1] V *vs.* the saturated calomel electrode, respectively); however, mphz$^{\bullet}$ remains in solution and does not contaminate

Table 5 Relevant magnetic, electrical and electronic data

Sample	ρ^a/Ω cm	$E_a{}^b$/eV	$E_{ct}{}^c$/eV	g	$\mu_{eff}/\mu_B{}^d$	$\Delta E_{o,r}{}^d$/V
1b $[NiL_2]$·dmphz·2MeCN	3.6×10^3	0.28	0.61	2.0030	0	+0.29
2b $[CoL_2]$·dmphz·2MeCN	4.2×10^5	0.26	*e*	2.0027	4.13	+0.34
1d $[NiL_2]$·$mphz^+$·2MeOH	5.5×10^6	0.43	*e*	2.0045	1.72	+0.24

[a] Measured at room temperature. [b] Thermal activation energy for conductivity, evaluated from the plot of ln σ *vs.* $1/T$. [c] Energy of the maximum of the charge-transfer band. [d] Difference between the oxidation potential of the donor and the reduction potential of the acceptor, calculated from their cyclovoltammograms. [e] Broad, intense, unresolved band.

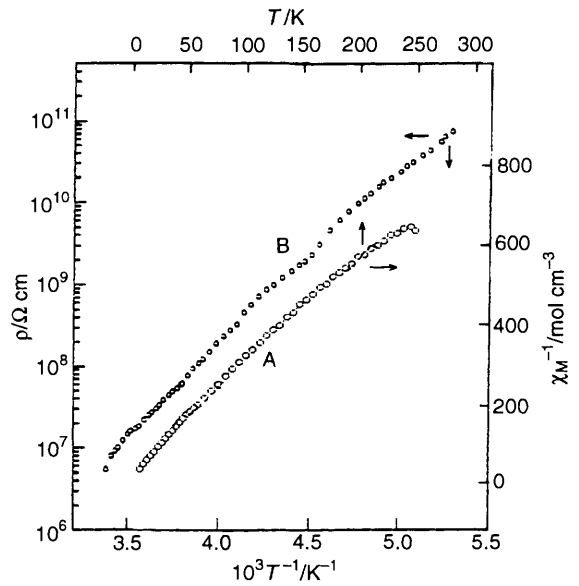

Fig. 8 Temperature dependence of the reciprocal molar susceptibility (A) and powder specific electrical resistivity (B) for compound **1d**

the final product because it does not give any insoluble c.t. complex with $[NiL_2]$ in the reaction mixture. This was proved by the direct reaction in methanol between the neutral constituents $[NiL_2]$ and mphz$^•$, prepared by potentiostatic reduction of *N*-methylphenazinium methanesulfate as described in the literature.[17] It is precisely because of the non-appearance of any precipitate in the last experiment that we believe **1d**, in spite of the positive $\Delta E_{o,r}$ (Table 5), is a simple radical anion salt, and must be regarded as an example of lattice stabilization of an otherwise neutral, soluble complex. The stoichiometry was obtained by elemental analysis, although an O:Ni atomic ratio of 2.13 instead of 2 was found. In our opinion the discrepancy is due to a non-homogeneity of the sample for the methanol content; indeed analysis on other samples gave an even higher O:Ni ratio, up to 3.89, while the mass spectrum did not reveal any species other than $[NiL_2]^{•-}$ and $mphz^+$.

Compound **1d** is paramagnetic with μ_{eff} corresponding to one unpaired electron per molecular formula at room temperature, and shows a weak antiferromagnetic coupling at low temperature (μ_{eff} = 1.21 μ_B at 7 K, Fig. 8). In marked contrast with $tcnq^{•-}$·$mphz^+$, **1d** is a poor conductor (Fig. 8), whose resistivity is two orders of magnitude higher than that of $[NiL_2]^{•-}$·$NEt_4{}^+$·4MeOH,[1] which is supposed to be a segregated-stack compound; it is thus expected to show a mixed stacking of a simple 1:1 ionic c.t. complex.

Finally, we would like to remove any doubt concerning the real nature of the cation in this ionic complex. One might expect the presence of the *N*-hydro-*N'*-methylphenazinylium radical cation (Hmphz$^{•+}$), to which $mphz^+$ could have been inadvertently converted in the electrochemical reduction, after adding both one electron and one proton; indeed both electron and proton transfer is a possibility occurring widely in phenazine-related molecules.[17] In that case, the very low conductivity of compound **1d** would be reasonable, given that the analogous salt $tcnq^{•-}$·Hmphz$^{•+}$ is a mixed-stacked,[18] very poor conductor ($\rho = 1.30 \times 10^6$ Ω cm);[19] however, this hypothesis can be excluded on the basis of the mass spectrum, which shows the peak at *m/z* 195 is more intense than that at *m/z* 196, while the reverse is usually observed and assumed as diagnostic for samples contaminated by Hmphz$^{•+}$.[20]

Experimental

Physical Measurements.—Infrared spectra were recorded on a Perkin Elmer 983 spectrometer. A Cary 5 instrument was used to record diffuse reflectance spectra on MgO-diluted samples. Magnetic measurements were performed on a commercial SQUID magnetometer (Quantum Design, H_{max} = 5 T); molar susceptibilities were corrected for intrinsic diamagnetism, estimated from Pascal's constants. EPR spectra were obtained with an X-band Varian spectrometer; the magnetic field was measured with a Bruker model B-NM.20 NMR gaussmeter. An AMEL system (model 472 polarograph, model 721 integrator, model 550 potentiostat) was used for the electrochemistry experiments. Fast-atom bombardment (FAB) mass spectra were obtained on a Shimadzu-Kratos Concept 1S spectrometer using *m*-nitrobenzyl alcohol as matrix. Electrical resistivity measurements of single crystals along the needle axis coinciding with the crystallographic *c* axis (**1b** and **2b**) and of pellets (**1d**) were performed by the two-probe method.

Materials.—Phenazine (from Fluka) was used as received. 5,10-Dimethyl-5,10-dihydrophenazine,[21] *N*-methylphenazinium methanesulfate[12] and $[NiL_2]$·4thf[1] were prepared according to the literature. All manipulations were carried out under a purified N_2 atmosphere using standard Schlenk techniques. Solvents were dried and degassed before use.

Syntheses.—$[NiL_2]$·2phz·2MeCN **1a**. A mixture of $[NiL_2]$·4thf (0.2 g, 0.123 mmol), phenazine (0.1 g, 0.555 mmol) and 1,2-dimethoxyethane–acetonitrile (2:8, 100 cm^3) was heated at reflux under N_2 for 30 min and then allowed to cool to room temperature. Black microcrystals of compound **1a** separated in quantitative yield. Suitable crystals for an X-ray structure determination were obtained after crystallization from the same solvent mixture as follows. A hot saturated solution was filtered and sealed in a vial under vacuum; on very slow cooling from 80 °C to room temperature over 4 d needle-like crystals separated. The elemental analyses were not reproducible, owing to the partial loss of MeCN when the sample was dried; however, the experimental X-ray powder diffraction patterns from freshly prepared samples were reproducible and in excellent agreement with the diffraction patterns calculated from single-crystal analysis.[22]

$[NiL_2]$·dmphz·2MeCN **1b**. A mixture of $[NiL_2]$·4thf (0.2 g, 0.123 mmol), 5,10-dimethyl-5,10-dihydrophenazine (0.1 g, 0.475 mmol) and methanol–acetonitrile (1:9, 100 cm^3) was stirred at room temperature for 3 h. The solution changed from dark blue to light yellow and black microcrystals of **1b** separated in quantitative yield. Crystals suitable for X-ray determination were obtained by slow interdiffusion of the filtered, clear solutions of the reagents in a standard H-shaped cell. As for

Table 6 Structure determination summary for the structures of **1a** and **1b***

Compound	**1a**	**1b**
Empirical formula	$C_{50}H_{26}N_{20}Ni$	$C_{40}H_{24}N_{18}Ni$
M	965.6	815.5
Crystal size/mm	1.5 × 0.3 × 0.3	1.0 × 0.3 × 0.2
Space group	$P2_1/n$	$P2_1/c$
a/Å	14.687(1)	12.975(5)
b/Å	21.364(2)	19.838(7)
c/Å	7.8208(6)	7.651(3)
β/°	110.958(6)	106.05(2)
U/Å^3	2291.7(3)	1892.6(12)
D_c/Mg m^{-3}	1.400	1.431
μ/mm^{-1}	0.499 (Mo-Kα)	1.194 (Cu-Kα)
F(000)	890	836
Diffractometer	Syntex $P2_1$	Rigaku AFC5R with a rotating anode
Radiation	Mo-Kα (λ = 0.710 69 Å)	Cu-Kα (λ = 1.5418 Å)
2θ range/°	3.0–55.0	5.0–120.0
Reflections collected	4784	3246
Independent reflections	3904 (R_{int} = 0.0453)	2611 (R_{int} = 0.0489)
Observed reflections	3359 [$I > 3\sigma(I)$]	2115 [$F > 6.0\sigma(F)$]
w^{-1}	$\sigma^2(F)$	$\sigma^2(F) + 0.0019F^2$
Final R, R'	0.0494, 0.0549	0.0553, 0.0789
Maximum, mean shift/σ	0.03, 0.01	0.25, 0.04
Maximum, minimum residue/e Å^{-3}	0.40, −0.45	0.55, −0.50

* Details in common: dark blue, prismatic crystals, monoclinic, $Z = 2$, θ–2θ scan type, highly oriented graphite crystal monochromator. $R = \Sigma||F_o| - |F_c||/\Sigma|F_o|$, $R' = [\Sigma w(|F_o| - |F_c|)^2/\Sigma w(F_o)^2]^{\frac{1}{2}}$.

the previous compound, the elemental analyses were not reproducible for the same reasons, in our opinion; however, we established both the reproducibility of the X-ray powder diffractograms of freshly prepared samples and their similarity with those calculated from a single crystal structure determinations.[22]

$[CoL_2]$·dmphz·2MeCN **2b**. Compound **2b** was synthesised similarly to the analogous nickel complex, with $[CoL_2]$·2dme (dme = dimethoxyethane) as starting material and acetonitrile as solvent; X-ray powder diffraction patterns showed it to be isomorphous and isostructural with **1b**.

$[NiL_2]^{\cdot-}$·mphz$^+$·2MeOH **1d**. Compound **1d** was obtained by galvanostatic electrolytic reduction, carried out in a two-compartment cell, separated by a glass-sintered disc (porosity 3), with two platinum-plate electrodes. The cathode compartment was filled with a solution of $[NiL_2]$·4thf (0.1 g, 0.123 mmol) in methanolic *N*-methylphenazinium methanesulfate (3.26×10^{-3} mol dm^{-3}, 100 cm^3) and the anode compartment filled with methanolic *N*-methylphenazinium methanesulfate (4.07×10^{-3} mol dm^{-3}). A constant current of 2 mA was applied and after 3 h the initial dark green solution faded and a black microcrystalline solid, firmly stuck to the cathode surface, was collected, washed with methanol and dried. Yield 0.08 g, 81% (Found: C, 57.60; H, 3.05; N, 28.60; Ni, 6.60; O, 3.85. Calc. for $C_{37}H_{23}N_{16}NiO_2$: C, 56.80; H, 2.95; N, 28.65; Ni, 7.50; O, 4.10%). Mass spectrum: (positive FAB) m/z 195 $[C_{13}H_{11}N_2]^+$; (negative FAB) m/z 521 $[Ni(C_{11}N_7H_2)_2 - H]^+$.

X-Ray Structure Determination.—Table 6 summarizes the relevant data for the crystal structures of **1a** and **1b**. For both compounds suitable single crystals were embedded in silicone grease in a glass capillary in the presence of mother-liquor, in order to avoid loss of the crystallization solvent.

During the data collection, a systematic decay reduced the standard-reflection intensity to 80% of the initial value for **1a**, and 60% for **1b**; diffraction data were therefore corrected for Lorentz, polarization, absorption (ψ-scan) and decay effect.

Unit-cell parameters were determined from 25 accurately centred high-angle reflections. The structures were solved by conventional heavy-atom methods and refined by full-matrix least-squares methods, with neutral scattering factors and anomalous dispersion factors taken from ref. 23. The hydrogen atoms were placed in calculated positions, with fixed isotropic thermal parameters, and restrained to ride on their associated atoms. Calculations were carried out using the SHELXTL PC[22] and SIR-CAOS[24] crystallographic program systems.

Additional material available from the Cambridge Crystallographic Data Centre comprises H-atom coordinates, thermal parameters and remaining bond lengths and angles.

X-Ray Powder Diffractometry.—Powder diffraction patterns were recorded on a computer-controlled Seifert XRD-3000 powder diffractometer with Cu-Kα graphite-monochromatized radiation. Data were collected by step-scanning in the range 2θ = 3–60°, with a step size of 0.01° and a count time of 10 s per step.

Acknowledgements

We thank Dr. A. Attanasio for EPR spectra, Mr. C. Veroli for drawings and technical assistance and the Progetto Finalizzato Materiali for partial financial support.

References

1 M. Bonamico, V. Fares, A. Flamini and N. Poli, *Inorg. Chem.*, 1991, **30**, 3081.
2 M. Bonamico, V. Fares, A. Flamini and N. Poli, *J. Chem. Soc., Dalton Trans.*, 1992, 3273.
3 M. Bonamico, V. Fares, A. Flamini and N. Poli, *J. Chem. Soc., Dalton Trans.*, 1993, 2073.
4 (*a*) M. Munakata, S. Kitagawa, N. Ujimaru, M. Nakamura, M. Maekawa and H. Matsuda, *Inorg. Chem.*, 1993, **32**, 826; (*b*) I. Goldberg and U. Shmueli, *Acta Crystallogr., Sect. B*, 1972, **29**, 440.
5 (*a*) I. Goldberg and I. Shmueli, *Acta Crystallogr., Sect. B*, 1973, **29**, 421; (*b*) M. Meneghetti, A. Girlando and C. Pecile, *J. Chem. Phys.*, 1985, **83**, 3124.
6 Z. G. Soos, H. J. Keller, K. Ludolf, J. Queckbörner, D. Wehe and S. Flandrois, *J. Chem. Phys.*, 1981, **74**, 5287.
7 T. Uchida, *Bull. Chem. Soc. Jpn.*, 1967, **40**, 2244.
8 K. Wozniak, B. Kariuki and W. Jones, *Acta Crystallogr., Sect. C*, 1991, **47**, 1113.
9 J. B. Torrance, J. E. Vazquez, J. J. Mayerle and V. Y. Lee, *Phys. Rev. Lett.*, 1981, **46**, 253.
10 J. B. Torrance, A. Gilardo, J. J. Mayerle, J. I. Crowley, V. Y. Lee, P. Batail and S. J. La Placa, *Phys. Rev. Lett.*, 1981, **47**, 1747;

J. Hubbard and J. B. Torrance, *Phys. Rev. Lett.*, 1981, **47**, 1750; P. Batail, S. J. La Placa, J. J. Mayerle and J. B. Torrance, *J. Am. Chem. Soc.*, 1981, **103**, 951; A. Gilardo, F. Marzola, C. Pecile and J. B. Torrance, *J. Chem. Phys.*, 1983, **79**, 1075.
11 I. Fujita and Y. Matsunaga, *Bull. Chem. Soc. Jpn.*, 1980, **53**, 267.
12 L. R. Melby, *Can. J. Chem.*, 1965, **43**, 1448.
13 A. Bencini and D. Gatteschi, *Transition Met. Chem.*, 1982, **8**, 1.
14 D. Attanasio, I. Collamati and C. Paul, *Inorg. Chem.*, 1985, **24**, 2746.
15 (*a*) C. J. Fritchie, jun., *Acta Crystallogr.*, 1966, **20**, 892; (*b*) A. J. Epstein, S. Etemad, A. F. Garito and A. J. Heeger, *Phys. Rev. B*, 1972, **5**, 952.
16 J. B. Torrance, *Acc. Chem. Res.*, 1979, **12**, 79.
17 W. Rubaszewska and Z. R. Grabowski, *J. Chem. Soc., Perkin Trans. 2*, 1975, 417.
18 B. Morosin, *Acta Crystallogr., Sect. B*, 1978, **34**, 1905.
19 L. B. Coleman, S. K. Khanna, A. F. Garito, A. J. Heeger and B. Morosin, *Phys. Lett. A*, 1972, **42**, 15.
20 D. J. Sandman, *J. Am. Chem. Soc.*, 1978, **100**, 5230; H. J. Keller, D. Nöthe, W. Moroni and Z. G. Soos, *J. Chem. Soc., Chem. Commun.*, 1978, 331.
21 H. Gilman and J. J. Dietrich, *J. Am. Chem. Soc.*, 1957, **79**, 6178.
22 SHELXTL PC Siemens Crystallographic Research System, Siemens Analytical X-Ray Instruments Inc., Madison, WI, 1990.
23 *International Tables for X-Ray Crystallography*, Kynoch Press, Birmingham, 1974, vol. 4.
24 M. Camalli, D. Capitani, G. Cascarano, S. Cerrini, C. Giacovazzo and R. Spagna, *Ital. Pat.*, 3543C/86, 1986.

Received 16*th June* 1993; *Paper* 3/03478J